

See discussions, stats, and author profiles for this publication at: <http://www.researchgate.net/publication/5381071>

# Chemically surface-modified carbon nanoparticle carrier for phenolic pollutants: Extraction and electrochemical determination of benzophenone-3 and triclosan

ARTICLE *in* ANALYTICA CHIMICA ACTA · JUNE 2008

Impact Factor: 4.51 · DOI: 10.1016/j.aca.2008.04.011 · Source: PubMed

---

CITATIONS

33

---

READS

34

9 AUTHORS, INCLUDING:



Lorena Vidal

University of Alicante

28 PUBLICATIONS 833 CITATIONS

SEE PROFILE



Antonio Canals

University of Alicante

111 PUBLICATIONS 2,006 CITATIONS

SEE PROFILE



Eleftheria Psillakis

Technical University of Crete

84 PUBLICATIONS 3,251 CITATIONS

SEE PROFILE



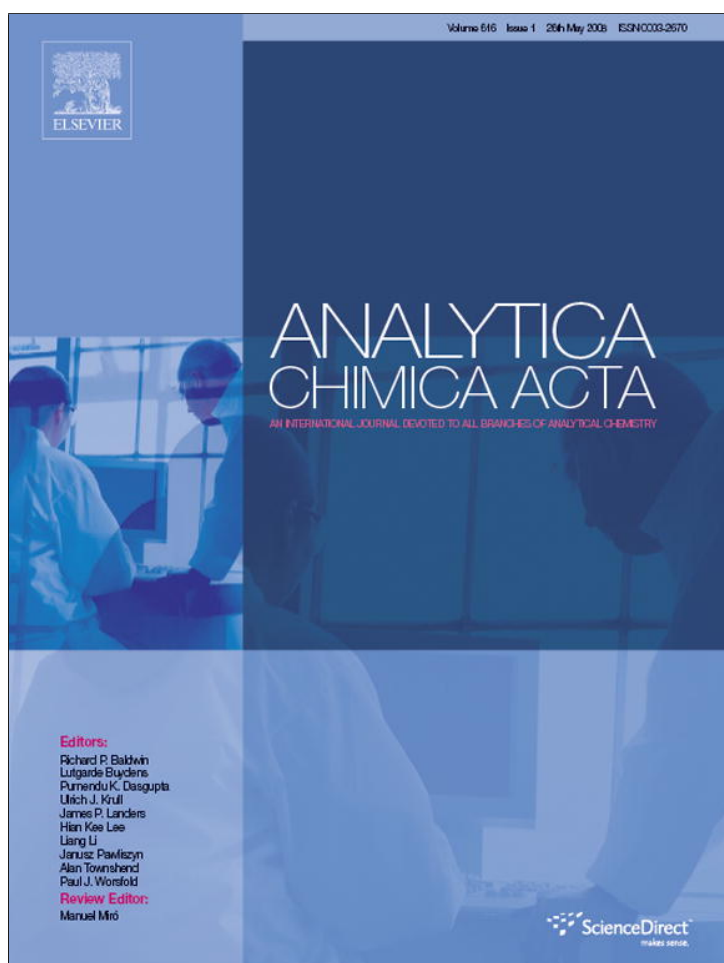
Karen Edler

University of Bath

114 PUBLICATIONS 1,227 CITATIONS

SEE PROFILE

Provided for non-commercial research and education use.  
Not for reproduction, distribution or commercial use.



This article appeared in a journal published by Elsevier. The attached copy is furnished to the author for internal non-commercial research and education use, including for instruction at the authors institution and sharing with colleagues.

Other uses, including reproduction and distribution, or selling or licensing copies, or posting to personal, institutional or third party websites are prohibited.

In most cases authors are permitted to post their version of the article (e.g. in Word or Tex form) to their personal website or institutional repository. Authors requiring further information regarding Elsevier's archiving and manuscript policies are encouraged to visit:

<http://www.elsevier.com/copyright>



ELSEVIER

available at [www.sciencedirect.com](http://www.sciencedirect.com)journal homepage: [www.elsevier.com/locate/aca](http://www.elsevier.com/locate/aca)

# Chemically surface-modified carbon nanoparticle carrier for phenolic pollutants: Extraction and electrochemical determination of benzophenone-3 and triclosan

Lorena Vidal<sup>a</sup>, Alberto Chisvert<sup>a</sup>, Antonio Canals<sup>a</sup>, Eleftheria Psillakis<sup>b</sup>, Alexei Lapkin<sup>c</sup>, Fernando Acosta<sup>c</sup>, Karen J. Edler<sup>d</sup>, James A. Holdaway<sup>d</sup>, Frank Marken<sup>d,\*</sup>

<sup>a</sup> Departamento de Química Analítica, Nutrición y Bromatología, Universidad de Alicante, P.O. Box 99, E-03080, Alicante, Spain

<sup>b</sup> Laboratory of Aquatic Chemistry, Department of Environmental Engineering, Technical University of Crete, Polytechniopolis, 73100 Chania-Crete, Greece

<sup>c</sup> Department of Chemical Engineering, University of Bath, Bath BA2 7AY, UK

<sup>d</sup> Department of Chemistry, University of Bath, Bath BA2 7AY, UK

## ARTICLE INFO

### Article history:

Received 2 February 2008

Received in revised form

2 April 2008

Accepted 6 April 2008

Published on line 11 April 2008

### Keywords:

Carbon nanoparticle

Voltammetry

Sensor

Extraction

Benzophenone-3

UV filter

Triclosan

Fungicide

Biocide

## ABSTRACT

Chemically surface-modified (tosyl-functionalized) carbon nanoparticles (Emperor 2000 from Cabot Corp.) are employed for the extraction and electrochemical determination of phenolic impurities such as benzophenone-3 (2-hydroxy-4-methoxybenzophenone) or triclosan (5-chloro-2-(2,4-dichlorophenoxy)phenol). The hydrophilic carbon nanoparticles are readily suspended and separated by centrifugation prior to deposition onto suitable electrode surfaces and voltammetric analysis. Voltammetric peaks provide concentration information over a 10–100  $\mu\text{M}$  range and an estimated limit of detection of ca. 10  $\mu\text{M}$  (or 2.3 ppm) for benzophenone-3 and ca. 20  $\mu\text{M}$  (or 5.8 ppm) for triclosan.

Alternatively, analyte-free carbon nanoparticles immobilized at a graphite or glassy carbon electrode surface and directly immersed in analyte solution bind benzophenone-3 and triclosan (both with an estimated Langmuirian binding constants of  $K \approx 6000 \text{ mol}^{-1} \text{ dm}^3$  at pH 9.5) and they also give characteristic voltammetric responses (anodic for triclosan and cathodic for benzophenone-3) with a linear range of ca. 1–120  $\mu\text{M}$ . The estimated limit of detection is improved to ca. 5  $\mu\text{M}$  (or 1.2 ppm) for benzophenone-3 and ca. 10  $\mu\text{M}$  (or 2.3 ppm) for triclosan. Surface functionalization is discussed as the key to further improvements in extraction and detection efficiency.

© 2008 Elsevier B.V. All rights reserved.

## 1. Introduction

The recently increased interest in the analysis of ingredients in pharmaceutical and personal care products (PCP) entering the environment is due to the need to monitor the build up of detectable and potentially harmful concentrations [1]. In addition to the well-recognized “priority” pollutants (pesticides,

polycyclic aromatic hydrocarbons, polychlorinated biphenyls, etc.) the release and transportation pathways of pharmaceutical and PCP ingredients into the aquatic environment has attracted particular attention [2,3]. The occurrence of pharmaceutical residues in the environment was recognized in 1976 [4] and confirmed in untreated sewage [5], surface water [6,7], groundwater, and in drinking water [3,8].

\* Corresponding author. Tel.: +44 1225 383694.

E-mail address: [f.marken@bath.ac.uk](mailto:f.marken@bath.ac.uk) (F. Marken).

0003-2670/\$ – see front matter © 2008 Elsevier B.V. All rights reserved.

doi:10.1016/j.aca.2008.04.011

Active ingredients of sunscreens in particular UV filters (which help to reduce skin damage from sunlight [9] and which are now part of many everyday products such as face creams, after shave products, shampoos, lipsticks, makeup formulations, etc.) are potentially toxic [10,11] and now widely found in the environment. Toxicity studies carried out *in vitro* or *in vivo* seem to indicate that some UV filters have significant estrogenic and/or antiandrogenic activity [12–14]. However, a study on changes in hormonal levels of human volunteers after applying certain sunscreen products seems to indicate that these are only minor effects [15]. Benzophenone-3 (BZ3), also known as oxybenzone or 2-hydroxy-4-methoxybenzophenone (see Fig. 1), is by far the most commonly used UV filter in cosmetic formulations worldwide [16].

Anti-microbial agents, which are used in many PCP products, can also be found in the environment. Triclosan, 5-chloro-2-(2,4-dichlorophenoxy)phenol (see Fig. 1), is an active ingredient in many household disinfectants and has been used extensively in improving environmental hygiene [17]. This chemical can also be found as an antiseptic component in medical products such as hand disinfecting soaps, medical skin creams, dental products, as well as in cosmetic products, deodorants, etc. As a consumer product ingredient, the majority of triclosan enters sewer systems and is transported to wastewater sewage treatment plants. Triclosan has been detected in sewage sludge, discharge effluent, receiving surface waters and sediments [16,18]. This compound has also been found in rivers, lakes and the open sea at  $\text{ngL}^{-1}$  levels [19–21]. The toxicity of triclosan on humans has been investigated for many years. The adverse effects include only mild itching and allergic redness on sensitive skins. Thus, triclosan is generally regarded as a low toxicity chemical [22,23]. However, under some conditions photodegradation of triclosan may lead to the formation of dioxin-type derivatives, chlorophenols, and chloroform [24,25], which may require monitoring.

This study focuses on the determination of the widely used ingredients benzophenone-3 and triclosan. The extraction and determination in water samples is the main aim of

this work. Previously, extraction and determination of these substances in water samples has been attempted by solid phase microextraction (SPME) [26–28], solid phase extraction (SPE) [24,29], ad-vesicle solid phase dispersion (ASPD) [30], stir-bar sorptive extraction (SBSE) [31], semi-permeable membrane devices (SPMDs) [32,33], liquid–liquid extraction (LLE) [34,35] and cloud point extraction (CPE) [36] coupled to chromatography, and by electrochemical methods [37–39].

A range of carbon materials, such as nanotubes and nanofibers have been used in solid phase extraction [40] and solid phase microextraction [41–43] usually as extractant phases for organic compounds. Carbon nanoparticles (or chemically surface functionalized carbon black) represent a very interesting carbon material which offers all the advantages of nanocarbons (extremely high surface area, adsorption sites, reactive surface sites, conductivity, etc.). Here a hydrophilic type of carbon nanoparticles with a tosyl functionalized surface is employed. These carbon nanoparticles are shown to provide a new pre-concentration or extraction tool/material for benzophenone-3 and for triclosan analytes in water samples. Two approaches are employed based on (i) the addition of carbon nanoparticles to the analyte solution, centrifugation, separation and transfer to an electrode surface and voltammetric determination and (ii) the immobilization of carbon nanoparticles at carbon electrode surfaces and direct voltammetric determination. The effectiveness of the two methods is compared and an estimate of the binding constant of the pollutants to the carbon nanoparticle surface is obtained.

## 2. Experimental

### 2.1. Chemical reagents

Benzophenone-3 (2-hydroxy-4-methoxybenzophenone, oxybenzone or BZ3) 98% was obtained from Aldrich (Steinheim, Germany). Triclosan (Irgasan, 5-chloro-2-(2,4-dichlorophenoxy)phenol) 97% was obtained from Fluka (Buchs, Switzerland). Carbon nanoparticles (ca.7.8 nm mean diameter, Emperor 2000) were obtained from Cabot Corporation (Dukinfield, United Kingdom). De-ionized water (resistivity not less than  $18\text{M}\Omega\text{cm}$ ) was obtained from a water purification system (Milli-Q Biocel A10) supplied by Millipore (Billerica, MA, USA). Potassium phosphate dibasic salt (98%) and potassium hydroxide pellets (85%) from Aldrich were used to prepare phosphate buffer solutions. Argon (Pureshield, BOC) was employed for de-aeration of electrolyte solutions. Experiments were conducted at  $22 \pm 2^\circ\text{C}$ .

### 2.2. Instrumentation

A three-electrode micro-Autolab III potentiostat system (Eco Chemie, NL) was employed to control the potential at the working electrode. The counter electrode was a platinum wire (0.5 mm diameter, 2 cm long) and a KCl saturated calomel electrode (SCE, Radiometer) was the reference electrode. The working electrode consisted of a 4.9-mm-diameter basal plane pyrolytic graphite inlaid disc ('Pyrocarbon', LeCarbone Ltd., Sussex, UK) or 3 mm diameter glassy carbon inlaid

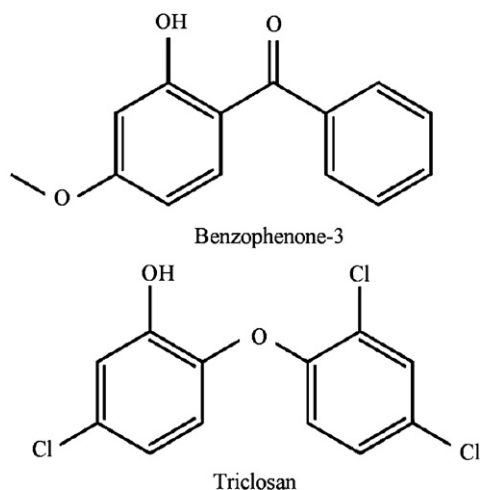


**Fig. 1** – Chemical structures of benzophenone-3 and triclosan.

disc (BAS Analytical). Working electrodes were polished on microcloth (Buehler) with 1  $\mu\text{m}$  alumina abrasive after measurements and prior to surface modification. A Hydrus 300 pH meter and FB 11012 ultrasonic bath (Fisher, UK) were used for the pH measurements and sample sonication, respectively. An Eppendorf (Hamburg, Germany) 5415D centrifuge was used to separate carbon nanoparticles from the analyte solution.

BET isotherm data were recorded on a Micrometrics ASAP 2010 BET V5.02 using a 5-point method. The sample was carefully dried at 150  $^{\circ}\text{C}$  under vacuum before analysis. Scanning electron microscopy images were obtained with a Leo 1530 Field Emission Gun Scanning Electron Microscope (FEGSEM) system after gold sputter coating of the sample. A SAXS/WAXS (simultaneous small-angle X-ray scattering and wide-angle X-ray scattering) pattern of the colloidal carbon nanoparticle solution (6 wt.% in water) was obtained on a SAXSess system using a PW3830 X-ray generator, and the X-ray image plates were observed using a PerkinElmer cyclone storage phosphor system. A colloidal solution in a capillary was employed and the patterns recorded in transmission mode with Cu K $\alpha$  radiation ( $\lambda = 1.5406 \text{ \AA}$ ) at 40 kV and 50 mA with an exposure time of 20 min. A background pattern from a clean capillary was subtracted and the data corrected for slit smearing before fitting the SAXS data (employing the package from the SANS group at NIST [44]). Spherical graphite particles of 1.9  $\text{g cm}^{-3}$  density were assumed.

### 2.3. Procedures

#### 2.3.1. Extraction with carbon nanoparticles and voltammetric determination

For the extraction process employing carbon nanoparticles in the analyte solution, 1 mg of the nanoparticles were added to 4 mL of the analyte solution (0.1 M phosphate buffer pH 9.5 containing either triclosan with  $\text{pK}_A \approx 8$  [45] or benzophenone-3 with  $\text{pK}_A \approx 9.5$  [46]; the buffer pH was selected to provide sufficient solubility for both systems and there is currently no systematic data available on the effect of the pH on the extraction process) and sonicated for 10 min. Next, 1 mL of this solution was centrifuged for 20 min at 8000 rpm. Once the nanoparticles with adsorbed analyte were separated from the suspension, 600  $\mu\text{L}$  of de-ionized water were added and the carbon nanoparticles were re-suspended with ultrasound. Finally, 40  $\mu\text{L}$  of the latter suspension (with 17  $\mu\text{g}$  carbon nanoparticles) were deposited onto the electrode surface and dried in an oven at 90  $^{\circ}\text{C}$ . Once the evaporation was completed, the electrode was introduced into the electrochemical cell (containing an aqueous 0.1 M phosphate buffer solution at pH 9.5) for voltammetric measurement. In some cases the extraction process was repeated (adding again 1 mg carbon nanoparticles into the remaining analyte solution) to explore the effectiveness of the extraction process.

#### 2.3.2. Immobilization of carbon nanoparticles and direct voltammetric determination

For the second process based on the in situ pre-concentration and measurement, films of carbon nanoparticles on the electrode surface were prepared by depositing 40  $\mu\text{L}$  drop of a

suspension, which contained 3 mg of carbon nanoparticles in 10 mL of de-ionized water (suspended by sonicating for 30 min). This electrode (with 12  $\mu\text{g}$  carbon nanoparticles) is then employed directly by immersion into a solution of analyte in aqueous 0.1 M phosphate buffer at pH 9.5, a 5-min pre-concentration at open circuit, and direct voltammetric measurement.

## 3. Results and discussion

### 3.1. Extraction of benzophenone-3 from aqueous media onto surface-modified carbon nanoparticles

Hydrophilic carbon nanoparticles offer an interesting adsorbent material for impurities in water and in particular for traces of aromatic compounds. The intrinsic electrical conductivity of carbon also provides the basis for the electrochemical detection of adsorbed species at the carbon nanoparticle

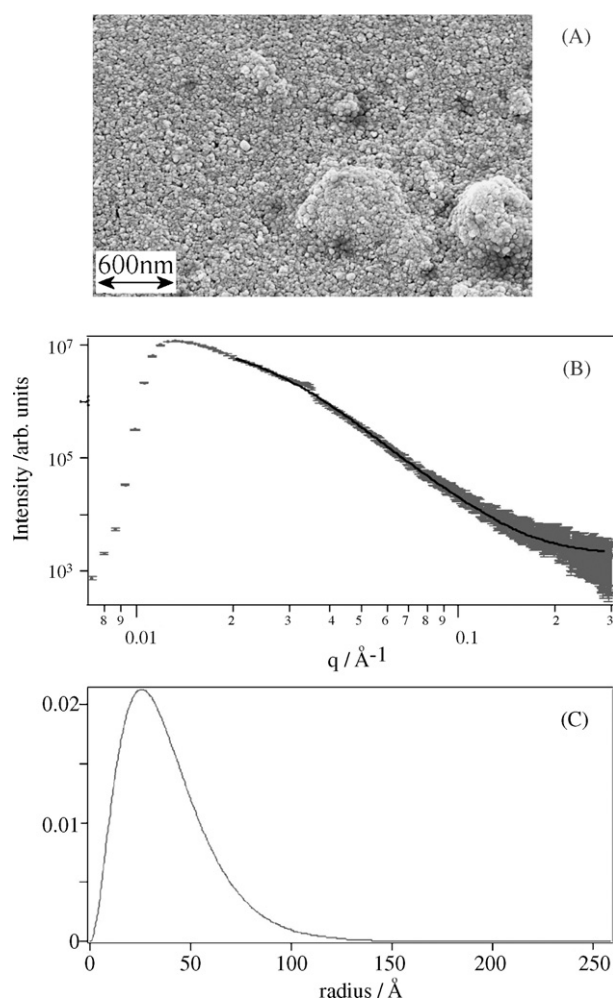


**Fig. 2 – (A) SEM image of carbon nanoparticles (gold sputter coated prior to imaging). (B) SAXS data (with error bars shown) for a 6% (w/v) carbon nanoparticle solution in water. The black line shows the theoretical fit assuming spherical particles with a mean radius of  $38 \pm 2 \text{ \AA}$  and a polydispersity of 0.57. (C) Schultz distribution calculated by fitting SAXS data.**

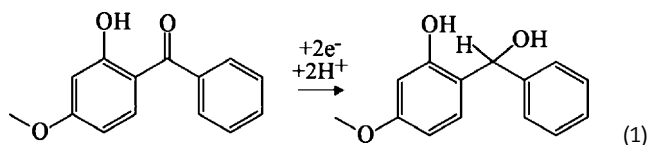
surface. Due to the surface functionalization of these nanoparticles with anionic tosyl groups they are readily dispersed (with ultrasound) and they offer a considerable surface area for extraction purposes.

Analysis of the surface area of the dry carbon nanoparticle powder gives a BET isotherm area of  $346 \text{ m}^2 \text{ g}^{-1}$  (5-point BET, see Section 2). When assuming spherical carbon particles with the density of graphite a radius of ca. 3.9 nm can be predicted based on this BET surface area. Scanning electron micrographs (see Fig. 2A) of the carbon nanoparticle material confirm a particle size in the order of 5 nm radius. Next, small-angle X-ray scattering experiments were carried out with a colloidal solution of 6% (w/v) carbon nanoparticles in water in order to further quantify the particle radius (see Fig. 2B). The mean particle radius 3.8 nm obtained by fitting the model of spherical particles is in excellent agreement with the BET prediction and the Schultz distribution shown in Fig. 2C represents a measure of the range of particle sizes encountered in this material.

Extraction experiments were first carried out in solution of analyte (benzophenone-3) in aqueous 0.1 M phosphate buffer pH 9.5. After addition of carbon nanoparticles, sonication, and centrifugation (see Section 2), a solid carbon nanoparticle residue is obtained with the analyte bound to the surface. A small amount of the re-suspended carbon nanoparticles ( $17 \mu\text{g}$ ) are then deposited onto an electrode surface and used for voltammetric analysis. Fig. 3A and B shows typical voltammetric responses observed at glassy carbon and at basal plane pyrolytic graphite electrodes.

Results obtained with the basal plane pyrolytic graphite electrode are slightly better probably due to the higher surface area and better adhesion of the carbon nanoparticles. It can be seen that with a scan rate of  $0.1 \text{ V s}^{-1}$  a well-defined reduction peak response occurs at a potential of  $-1.48 \text{ V}$  versus SCE. This reduction response is consistent with literature reports

[47,48] and it can be identified as the two-electron reduction of benzophenone-3 (see eq. (1)).



Both, the peak current and the peak charge (see Fig. 3C and D) are dependent on the concentration of benzophenone-3. The approximately linear dependence suggests that under conditions chosen in this experiment, the surface of the carbon nanoparticles is far from saturated. The limit of detection is governed by the considerable capacitive background current and can be estimated from the plot in Fig. 3D as  $10 \mu\text{M}$  (or 2.3 ppm).

During the extraction process the solution is depleted of benzophenone-3. A repeat extraction employing the same analyte solution (adding another 1 mg into 4 mL) shows only very low signals (see Fig. 3A and B) consistent with only traces of benzophenone-3 remaining in solution after the first extraction. In fact the ratio of the peak currents observed in the first and the second extraction can be employed to derive an approximate value for the binding constant (vide infra).

### 3.2. Extraction of triclosan from aqueous media onto surface-modified carbon nanoparticles

Next, extraction experiments with triclosan (5-chloro-2-(2,4-dichloro-phenoxy)-phenol) are reported. Triclosan is soluble in alkaline aqueous media and used here in 0.1 M phosphate buffer solution at pH 9.5. Carbon nanoparticles added into the solution, sonicated for 10 min, and then extracted by centrifu-

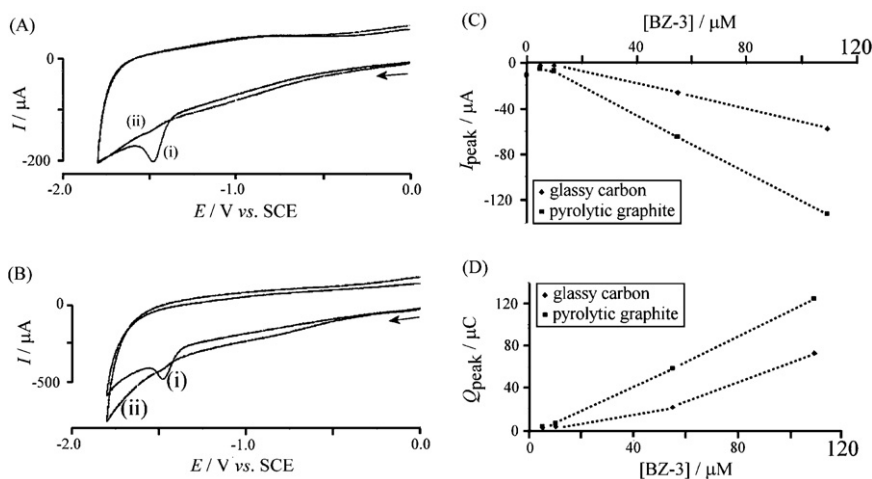


**Fig. 3 – (A) Cyclic voltammograms (scan rate  $0.1 \text{ V s}^{-1}$ ) obtained at a 3-mm-diameter glassy carbon electrode for the reduction of benzophenone-3 immobilized at carbon nanoparticles ( $17 \mu\text{g}$  immobilized at the electrode surface) after extraction from a solution of  $109 \mu\text{M}$  benzophenone-3 in aqueous 0.1 M phosphate buffer pH 9.5. Scan (i) shows the voltammetric response after the first extraction and scan (ii) shows the response after a consecutive second extraction. (B) Voltammetric data for the same experiment carried out with a 4.9-mm-diameter basal plane pyrolytic graphite electrode. (C) Plot of the cathodic peak current for the reduction of benzophenone-3 versus the starting concentration in the analyte solution. (D) Plot of the cathodic peak charge for the reduction of benzophenone-3 versus the starting concentration in the analyte solution.**

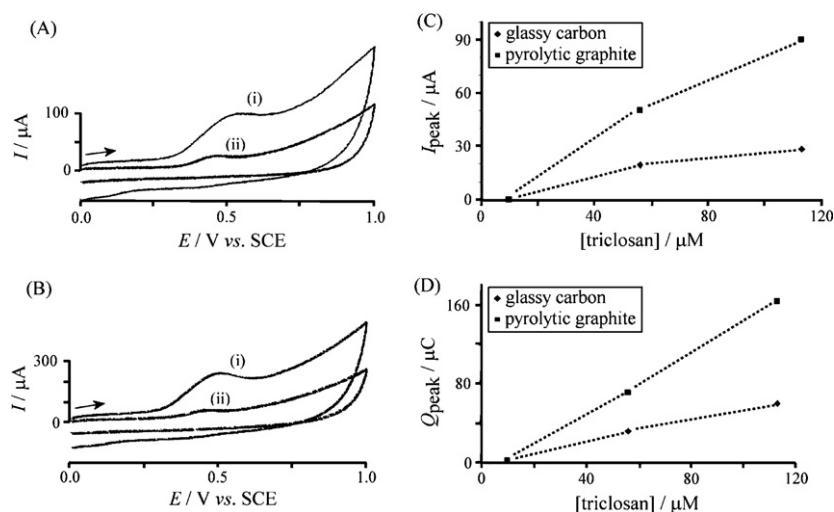
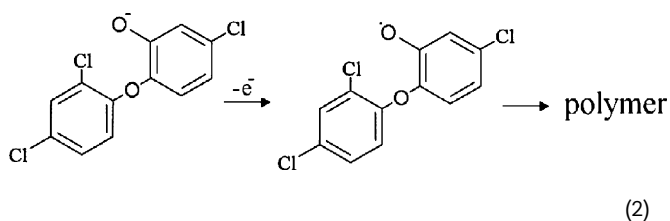


**Fig. 4** – (A) Cyclic voltammograms (scan rate  $0.1 \text{ V s}^{-1}$ ) for the oxidation of triclosan adsorbed onto carbon nanoparticles (1 mg of carbon nanoparticles in 4 mL of  $113 \mu\text{M}$  triclosan in  $0.1 \text{ M}$  phosphate buffer pH 9.5) and immobilized onto a 3-mm-diameter glassy carbon electrode ( $17 \mu\text{g}$  carbon nanoparticles were deposited by evaporation of an aqueous suspension, see Section 2). The voltammetric responses are shown for the first extraction process (i) and for the second extraction process (ii). (B) The same experiment conducted with a 4.9-mm-diameter basal plane pyrolytic graphite electrode. (C) Plot of the peak current for the triclosan oxidation versus analyte concentration. (D) Plot of the charge under the triclosan oxidation peak versus analyte concentration.

gation were deposited onto glassy carbon (Fig. 4A) and basal plane pyrolytic graphite (Fig. 4B) electrodes.

The characteristic oxidation response for triclosan at  $0.5 \text{ V}$  versus SCE is observed and the peak current and the peak charge (see Fig. 4C and D) are found to be proportional to the analyte concentration. The oxidation is chemically irreversible and has been proposed to follow a one-electron pathway [49] (see eq. (2)).



The peak observed after the second extraction (see scan (ii) in Fig. 4A and B) is considerably lower suggesting under the conditions of the experiment an approximately 90% effective removal of triclosan from the solution (the ratio of first extraction peak current to second extraction peak current is approximately 10). The limit of detection under these conditions can be estimated from the plot in Fig. 4D as ca.  $20 \mu\text{M}$  (or  $5.8 \text{ ppm}$ ).

In both extraction experiments, for benzophenone-3 and for triclosan, the ratio of the peak current after the first extraction and the peak current after the second consecutive extraction is approximately 10 suggesting similar binding ability under these conditions. It is interesting to evaluate this parameter by introducing a simple Langmuir binding model

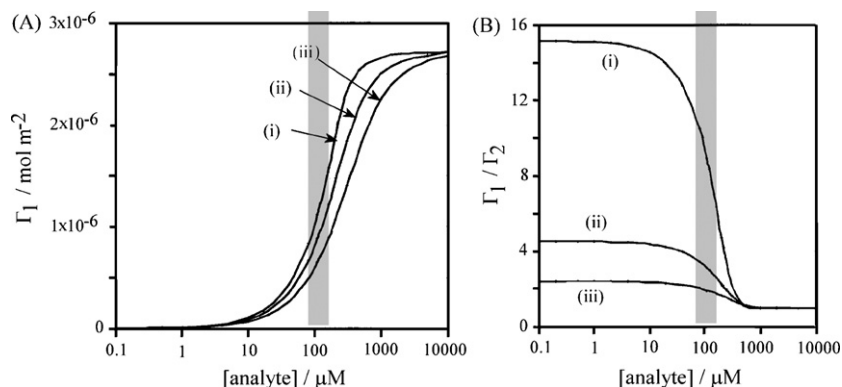


**Fig. 5** – (A) Plot of the surface coverage during the first extraction step assuming (i)  $K = 60,000 \text{ mol}^{-1} \text{ dm}^3$ , (ii)  $K = 15,000 \text{ mol}^{-1} \text{ dm}^3$ , and (iii)  $K = 6000 \text{ mol}^{-1} \text{ dm}^3$  ( $V = 4 \times 10^{-6} \text{ m}^3$ ,  $A = 0.346 \text{ m}^2$ ,  $\Gamma_0 = 2.7 \times 10^{-6} \text{ mol m}^{-2}$  assuming a molecular area of ca.  $2 \times 10^{-19} \text{ m}^2$ ). (B) Plot of the ratio of surface coverages in extractions 1 and 2 versus the initial analyte concentration. The grey zone is indicating the experimental value of  $109 \mu\text{M}$  (see above).

(eq. (3)).

$$\frac{\Gamma_1}{\Gamma_0} = \frac{Kc_1}{1 + Kc_1} \quad (3)$$

In this equation the surface coverage,  $\Gamma_1$ , is given by the available surface sites,  $\Gamma_0$ , the binding constant,  $K$ , and the solution concentration after the first extraction,  $c_1$ . After equilibration the concentration  $c_1 = c_0 - (\Gamma_1 A/V)$  will be lower than the initial concentration  $c_0$  due to the surface coverage  $\Gamma_1$  multiplied by the carbon nanoparticle area  $A$  and divided by the solution volume  $V$ . The parameter  $c_1$  in eq. (3) is substituted and the expression resolved for  $\Gamma_1$ . The resulting expression for the coverage (which is assumed to be proportional to the peak current) as a function of the initial concentration is a quadratic expression (see eq. (4)).

$$\Gamma_1 = \left( \frac{c_0 V}{2A} + \frac{V}{2AK} + \frac{\Gamma_0}{2} \right) - \sqrt{\left( \frac{c_0 V}{2A} + \frac{V}{2AK} + \frac{\Gamma_0}{2} \right)^2 - \frac{c_0 \Gamma_0 V}{A}} \quad (4)$$

Fig. 5A shows a plot of the surface coverage predicted under the experimental conditions ( $V = 4 \times 10^{-6} \text{ m}^3$ ,  $A = 0.346 \text{ m}^2$ ,  $\Gamma_0 = 2.7 \times 10^{-6} \text{ mol m}^{-2}$  assuming a molecular area of ca.  $2 \times 10^{-19} \text{ m}^2$ ) and for three different binding constants. An expression similar to eq. (4) but for the second extraction (using  $c_2 = c_0 - (\Gamma_1 A/V) - (\Gamma_2 A/V)$ ) can be employed similarly to express the surface coverage  $\Gamma_2$ . The plot in Fig. 5B shows the ratio of coverage for the first and second extraction (which is assumed to be approximately equivalent to the ratio of the peak currents observed for the first and second extraction). As expected, at very high analyte concentration the ratio is unity but at very low concentration the ratio becomes constant and proportional to the binding constant.

Based on the ratio of the peak currents for the first and second extraction of approximately 10 for an analyte concentration of  $109 \mu\text{M}$  (see Figs. 3A and B and 4A and B), the binding constant can be estimated from Fig. 5B as  $K \approx 60,000 \text{ mol}^{-1} \text{ dm}^3$  (curve (i)). However, this value has to be regarded only as a higher limit due to considerable uncertainty in the peak current data. It can be seen that plots in Figs. 4C and D and 3C and D do not go through the origin, and therefore, low concentration peaks are smaller than predicted from a simple linear relationship. Also, the charge under the voltammetric peaks is lower than that expected based on the simple Langmuir model. It seems, therefore, likely that after immersion of the modified electrode into the analyte-free buffer solution gradual loss of analyte or loss of some carbon material from the surface occurs. In the next section an alternative approach to quantitative analysis of analyte binding is investigated.

### 3.3. Voltammetric determination of benzophenone-3 at carbon nanoparticle modified electrodes

Next, voltammetric experiments were conducted with the carbon nanoparticles directly immobilized at the electrode surface which is then immersed directly into the analyte solution (see Section 2). In this way, the carbon nanoparticles act as the adsorption medium and enhanced voltammetric signals are observed without changing the solution. In stagnant solu-

tion, carbon nanoparticles were found to remain immobilized at the electrode surface and a typical set of voltammograms for the reduction of benzophenone-3 is shown in Fig. 6A. A well-defined chemically irreversible reduction response is observed in the presence of  $12 \mu\text{g}$  carbon nanoparticles and for concentrations of 5, 10, 55, and  $109 \mu\text{M}$  benzophenone-3 in aqueous  $0.1 \text{ M}$  phosphate buffer pH 9.5. In the absence of the carbon nanoparticles a much smaller reduction response is detected.

The amount of carbon nanoparticles employed in these experiments is crucial, and therefore, several sets of experiments were conducted to optimize this parameter. Data in Fig. 6B shows the normalized peak current (the peak current divided by the capacitive current) for the benzophenone-3 reduction. Perhaps surprisingly, this value is reduced for higher loading which suggests an increased capacitive background with only little improvement in the faradic signal. It seems possible that for a higher loading with carbon nanoparticles the time for uptake of analyte increases significantly

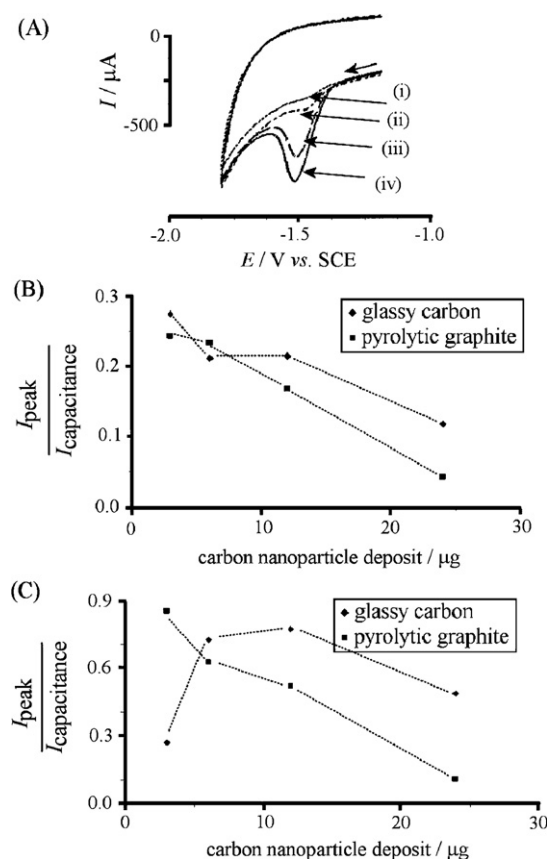
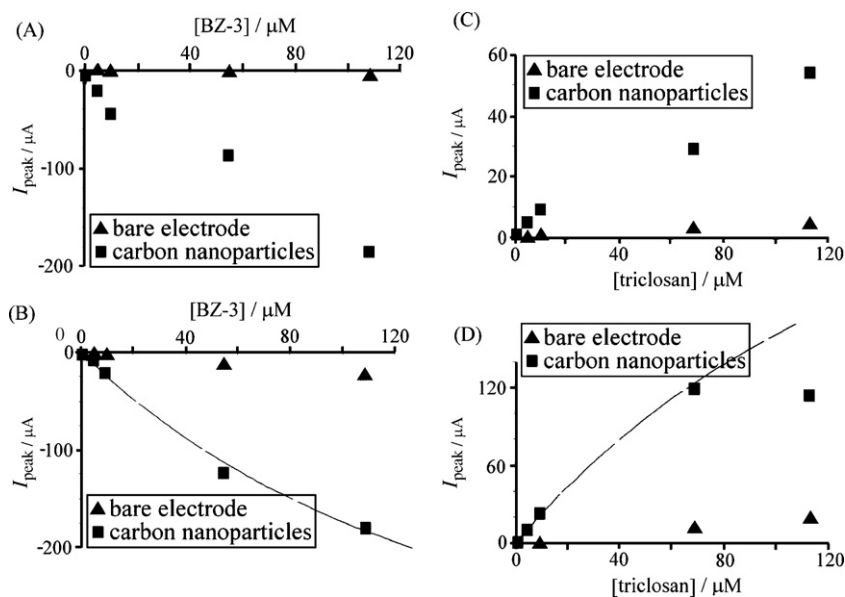


Fig. 6 – (A) Cyclic voltammograms (scan rate  $0.1 \text{ V s}^{-1}$ ) for the reduction of benzophenone-3 at a 4.9-mm-diameter basal plane pyrolytic graphite electrode with  $12 \mu\text{g}$  carbon nanoparticles immobilized and immersed in (i)  $5 \mu\text{M}$ , (ii)  $10 \mu\text{M}$ , (iii)  $55 \mu\text{M}$ , and (iv)  $109 \mu\text{M}$  benzophenone-3 in  $0.1 \text{ M}$  phosphate buffer pH 9.5. (B) Plot of the normalized peak current (peak current/capacitive current) for the reduction of  $10 \mu\text{M}$  benzophenone-3 in  $0.1 \text{ M}$  phosphate buffer pH 9.5 versus the amount of carbon nanoparticles deposited at the electrode surface. (C) Plot of the normalized peak current (peak current/capacitive current) for the oxidation of  $10 \mu\text{M}$  triclosan in  $0.1 \text{ M}$  phosphate buffer pH 9.5 versus the amount of carbon nanoparticles deposited at the electrode surface.



**Fig. 7 – (A)** Plot of the voltammetric peak current (scan rate  $0.1 \text{ V s}^{-1}$ ) for the reduction of benzophenone-3 at a 3-mm-diameter glassy carbon electrode with  $12 \mu\text{g}$  carbon nanoparticles versus concentration in aqueous  $0.1 \text{ M}$  phosphate buffer pH 9.5. **(B)** Plot for data obtained at a 4.9-mm-diameter basal plane pyrolytic graphite electrode. The line is indicating a Langmuir isotherm trend line with  $K \approx 6000 \text{ mol}^{-1} \text{ dm}^3$ . **(C)** Plot of the voltammetric peak current (scan rate  $0.1 \text{ V s}^{-1}$ ) for the oxidation of triclosan at a 3-mm-diameter glassy carbon electrode with  $12 \mu\text{g}$  carbon nanoparticles versus concentration in aqueous phosphate buffer pH 9.5. **(D)** Plot for data obtained at a 4.9-mm-diameter basal plane pyrolytic graphite electrode. The line is indicating a Langmuir isotherm trend line with  $K \approx 6000 \text{ mol}^{-1} \text{ dm}^3$ .

and only the capacitive current is increased. Therefore, under conditions of the experiment a carbon nanoparticle deposit of  $12 \mu\text{g}$  was chosen as a compromise to provide good sensitivity for both glassy carbon and basal plane pyrolytic graphite at low concentration of analyte.

Next, the effect of the benzophenone-3 concentration on the reduction response is investigated. Data in Fig. 7A and B demonstrate a systematic change in the peak current with concentration for both glassy carbon and graphite electrodes.

It is possible to obtain information about the binding constant (at least approximate) of benzophenone-3 onto the carbon nanoparticle substrate by fitting a Langmuir isotherm model into the data point in Fig. 7B. For a binding constant of  $K \approx 60000 \text{ mol}^{-1} \text{ dm}^3$  (vide supra) the deviation in all data points is considerable but for  $K \approx 6000 \text{ mol}^{-1} \text{ dm}^3$  a reasonable agreement between theory and experiment is achieved. The higher binding constant obtained above with the centrifugation procedure appears less accurate due to non-linearity at low analyte concentration (vide supra), and therefore,  $K \approx 6000 \text{ mol}^{-1} \text{ dm}^3$  appears to be the more accurate result. In order to improve the considerable uncertainty in this estimate a more extensive data set (over a wider concentration range and for different carbon loadings) would be required. For analytical purposes, for this experiment the limit of detection can be estimated from the plot in Fig. 7B as ca.  $5 \mu\text{M}$  (or  $1.2 \text{ ppm}$ ).

### 3.4. Voltammetric determination of triclosan at carbon nanoparticle modified electrodes

The adsorption of triclosan from  $0.1 \text{ M}$  phosphate solution (pH 9.5) onto carbon nanoparticles is also observed when carbon

nanoparticles are immobilized at the electrode surface and measurements are conducted in stagnant solution. Data in Fig. 6C suggest that good results are obtained with a  $12 \mu\text{g}$  carbon nanoparticle deposit for both glassy carbon and for basal plane pyrolytic graphite electrodes. Fig. 7C and D gives concentration dependent peak currents which suggest close to linear dependence and an approximate limit of detection at  $10 \mu\text{M}$  (or  $2.3 \text{ ppm}$ , estimated from the plot in Fig. 7D). The binding constant  $K \approx 6000 \text{ mol}^{-1} \text{ dm}^3$  is very similar for triclosan and for benzophenone-3.

## 4. Summary

It has been shown that  $7.8 \text{ nm}$  diameter carbon nanoparticles (surface functionalized with tosyl groups) effectively bind polyaromatic phenols from aqueous media. Two experimental approaches have been investigated: (i) the extraction of aromatic phenols onto carbon nanoparticles followed by deposition onto electrodes and (ii) the adsorption of aromatic phenols directly onto carbon nanoparticles immobilized at electrodes. The extraction process has been demonstrated to be highly effective. However, details of the adsorption mechanism and the molecular interaction between analyte and carbon nanoparticles are currently not fully understood. In both cases the limit of detection is in the  $5\text{--}20 \mu\text{M}$  (or  $2\text{--}6 \text{ ppm}$ ) range, but the detection with carbon nanoparticles immobilized at basal plane pyrolytic graphite is the method of choice for both triclosan and benzophenone-3 analytes. In future, the surface functionalization of the carbon nanoparticles could be improved to further enhance

the binding effects or the binding specificity. For example, naphthylsulfonate functionalization or introducing further cationic components could dramatically change the extraction behavior of the carbon nanoparticle material. Therefore, surface-modified/functionalized carbon nanoparticle based materials are promising reagents for the removal and the detection of redox active aromatics.

## Acknowledgements

The authors thank the COST network (Action D32, working group D32/005/04 "Microwave and Ultrasound Activation in Chemical Analysis) for support of this work. We thank Cabot Corporation for generous supply with carbon nanomaterials. L.V. thanks "Vicerrectorado de Investigación, Desarrollo e Innovación" (University of Alicante) for the financial support

## REFERENCES

- [1] D. Barcelo, P. Grathwohl, K. Jones, K.U. Totsche, Identification of priority compound classes. SOVA Report 1: Integrated Soil and Water Protection (2003) p. 5.
- [2] C.G. Daughton, T.A. Ternes, *Environ. Health Persp.* 107 (1999) 907.
- [3] M.E. Lindsey, M. Meyer, E.M. Thurman, *Anal. Chem.* 73 (2001) 4640.
- [4] A.W. Garrison, J.D. Pope, F.R. Allen, in: C.H. Keith (Ed.), Identification and Analysis of Organic Pollutants in Water, Ann Arbor Science Publication, Ann Arbor, MI, 1976, p. pp. 517.
- [5] R. Hirsch, T.A. Ternes, K. Haberer, K.-L. Kratz, *Sci. Total Environ.* 225 (1999) 109.
- [6] H. Buser, T. Poiger, M.D. Müller, *Environ. Sci. Technol.* 32 (1998) 3449.
- [7] T.A. Ternes, *Water Res.* 32 (1998) 3245.
- [8] C. Potera, *Environ. Health Persp.* 108 (2000) A446.
- [9] A. Chisvert, A. Salvador, UV Filters in Sunscreens and Other Cosmetics. Regulatory Aspects and Analytical Methods, in Analysis of Cosmetic Products, Elsevier, Amsterdam, 2007.
- [10] L.G. Dimosthenis, A. Salvador, A. Chisvert, *TRAC Trends Anal. Chem.* 26 (2006) 360.
- [11] S.D. Richardson, *Anal. Chem.* 79 (2007) 4295.
- [12] T. Suzuki, S. Kitamura, R. Khota, K. Sugihara, N. Fujimoto, S. Ohta, *Toxicol. Appl. Pharmacol.* 203 (2005) 9.
- [13] M. Schlumpf, P. Schmid, S. Durrer, M. Conscience, K. Maerkel, M. Henseler, M. Gruetter, I. Herzog, S. Reolon, R. Ceccatelli, O. Faass, E. Stutz, H. Jarry, W. Wuttke, W. Lichtensteiger, *Toxicology* 205 (2004) 113.
- [14] T. Hayashi, Y. Okamoto, K. Ueda, N. Kojima, *Toxicol. Lett.* 167 (2006) 1.
- [15] N.R. Janjua, B. Mogensen, A.M. Andersson, J.H. Petersen, M. Henriksen, N.E. Skakkebaek, H.C. Wulf, *J. Invest. Dermatol.* 123 (2004) 57.
- [16] A.M. Peck, *Anal. Bioanal. Chem.* 386 (2006) 907.
- [17] T. Okumura, Y. Nishikawa, *Anal. Chim. Acta* 325 (1996) 175.
- [18] W. Hua, E.R. Bennett, R.J. Letcher, *Environ. Int.* 31 (2005) 621.
- [19] D.W. Kolpin, M. Skopec, M.T. Meyer, E.T. Furlong, S.D. Zaugg, *Sci. Total Environ.* 328 (2004) 119.
- [20] P.M. Thomas, G.D. Foster, *J. Environ. Sci. Health A* 39 (2004) 1969.
- [21] D.W. Kolpin, E.T. Furlong, M.T. Meyer, E.M. Thurman, S.D. Zaugg, L.B. Barber, H.T. Buxton, *Environ. Sci. Technol.* 36 (2002) 1202.
- [22] A. Lindström, I.J. Buerge, T. Poiger, P. Bergqvist, M.D. Müller, H. Buser, *Environ. Sci. Technol.* 36 (2002) 2322.
- [23] C. Tixier, H. Singer, S. Canonica, S. Müller, *Environ. Sci. Technol.* 36 (2002) 3482.
- [24] L. Sanchez-Prado, M. Llompart, M. Lores, M. Fernandez-Alvarez, C. Garcia-Jares, R. Cela, *Anal. Bioanal. Chem.* 384 (2006) 1548.
- [25] D.E. Latch, J.L. Packer, W.A. Arnold, K. McNeill, *J. Photochem. Photobiol. A* 158 (2003) 63.
- [26] T. Felix, B.J. Hall, J.S. Brodbelt, *Anal. Chim. Acta* 371 (1998) 195.
- [27] D.A. Lambropoulou, D.L. Giokas, V.A. Sakkas, T.A. Albanis, M.I. Karayannis, *J. Chromatogr. A* 967 (2002) 243.
- [28] P. Canosa, I. Rodriguez, E. Rubi, R. Cela, *Anal. Chem.* 79 (2007) 1675.
- [29] R. Gibson, E. Becerril-Bravo, V. Silva-Castro, B. Jiménez, *J. Chromatogr. A* 1169 (2007) 31.
- [30] N.A. Parisis, D.L. Giokas, A.G. Vlessidis, N.P. Evmiridis, *J. Chromatogr. A* 1097 (2005) 17.
- [31] M. Kawaguchi, R. Ito, N. Endo, N. Sakui, N. Okanouchi, K. Saito, N. Sato, T. Shiozaki, H. Nakazawa, *Anal. Chim. Acta* 557 (2006) 272.
- [32] M.E. Balmer, H.R. Buser, M.D. Muller, T. Poiger, *Environ. Sci. Technol.* 39 (2005) 953.
- [33] A. Lindstrom, I.J. Buerge, T. Poiger, P.A. Bergqvist, M.D. Muller, H.R. Buser, *Environ. Sci. Technol.* 36 (2002) 2322.
- [34] L. Vidal, A. Chisvert, A. Canals, A. Salvador, *J. Chromatogr. A* 1174 (2007) 95.
- [35] H.K. Jeon, Y. Chung, J.C. Ryu, *J. Chromatogr. A* 1131 (2006) 192.
- [36] D.L. Giokas, V.A. Sakkas, T.A. Albanis, D.A. Lambropoulou, *J. Chromatogr. A* 1077 (2005) 19.
- [37] M. Amiri, S. Shahrokhian, E. Psillakis, F. Marken, *Anal. Chim. Acta* 593 (2007) 117.
- [38] M.A. Ghanem, R.G. Compton, B.A. Coles, E. Psillakis, M.A. Kulandainathan, F. Marken, *Electrochim. Acta* 53 (2007) 1092.
- [39] L.-H. Wang, *Electroanalysis* 14 (2002) 773.
- [40] Q. Zhou, W. Wang, J. Xiao, *Anal. Chim. Acta* 559 (2006) 200.
- [41] X. Liu, Y. Ji, Y. Zhang, H. Zhang, M. Liu, *J. Chromatogr. A* 1165 (2007) 10.
- [42] T. Sun, J. Jia, N. Fang, Y. Wang, *Anal. Chim. Acta* 530 (2005) 33.
- [43] J.-X. Wang, D.-Q. Jiang, Z.-Y. Gu, X.-P. Yan, *J. Chromatogr. A* 1137 (2006) 8.
- [44] S.R. Kline, *J. Appl. Cryst.* 39 (2006) 895.
- [45] A. Safavi, N. Maleki, H.R. Shahbaazia, *Bull. Electrochem.* 21 (2005) 229.
- [46] G.T. Castro, O.S. Giordano, S.E. Blanco, *J. Mol. Struct. -Theochem.* 626 (2003) 167.
- [47] A.P. da Silva, M.A.G. Trindade, V.S. Ferreira, *Talanta* 68 (2006) 679.
- [48] M. Chandrasekaran, M. Noel, V. Krishnan, *Collect. Czech. Chem. Commun.* 56 (1991) 2055.
- [49] R.M. Pemberton, J.P. Hart, *Anal. Chim. Acta* 390 (1999) 107.